Hydraulics of Dams and River Structures – Yazdandoost & Attari (eds)
© 2004 Taylor & Francis Group, London, ISBN 90 5809 632 7

Stepped spillways for embankment dams. Review, progress and development in overflow hydraulics

H. Chanson & C.A. Gonzalez
The University of Queensland, Dept. of Civil Eng., Brisbane, Australia

ABSTRACT: In recent years a number of embankments were designed with concrete overtopping protection shaped in a stepped fashion. During large overflows on stepped chutes, there is no skin friction between mainstream and steps, and flow resistance is basically form drag. Alterations of flow recirculation and of fluid exchanges between free-stream and cavity flow are discussed in this study. A comprehensive series of air-water flow measurements on embankment dam stepped chute are presented. The introduction of vanes demonstrates turbulence manipulation and form drag modification that could lead to more efficient designs.

1 INTRODUCTION

In recent years, the design floods of a number of dams were re-evaluated and the revised flows were often larger than those used for the original designs. In many cases, occurrence of the revised design floods would result in dam overtopping because of the insufficient storage and spillway capacity of the existing reservoir. This is unacceptable for embankment structures without overtopping protection systems. During the last three decades, a number of embankment dam spillways were designed with concrete overtopping protection shaped in a stepped fashion (e.g. CHANSON and TOOMBES 2001, CHANSON 2001 pp. 220–230). Although some overflow systems were made of timber cribs, sheet-piles, riprap and gabions, and reinforced earth, recent structures were designed with concrete slabs and formed concrete (CHANSON 2001). During the 1990s, the construction of secondary stepped spillways for embankment accounted for nearly two-thirds of dam construction in USA (DITCHEY and CAMPBEL 2000). The preferred construction method was roller compacted concrete overlays placed on the downstream slope (Fig. 1).

While most modern stepped spillways were designed as prismatic rectangular chutes with flat horizontal steps, recent studies hinted means to enhance the rate of energy dissipation (see next paragraph). In skimming flows on stepped chutes, there is no skin friction between free-stream

Figure 1. Stepped overflow protection system for a detention basin in west Las Vegas under construction (Courtesy of M.R. DELCAU and USACE-LA District).

and stepped invert, but at the step edges which are hydrodynamic singularities. Flow resistance is basically form drag. Alterations of flow recirculation and of fluid exchanges between free-stream and cavity flow may affect drastically the form losses and in turn the rate of energy dissipation. In the present study, new experiments were conducted at near full-scale with a 22° slope. Interactions between free-surface and cavity recirculation were thoroughly investigated in the skimming flow regime, while the effects of turbulence manipulation were systematically detailed.

1.1 *Energy dissipation enhancement: prototype and laboratory experience*

During the 19th century, overflow stepped spillways were selected frequently with nearly one third of the dams built in USA being equipped with a stepped cascade (e.g. SCHUYLER 1909, WEGMANN 1922, CHANSON 2001). Most structures had flat horizontal steps (e.g.

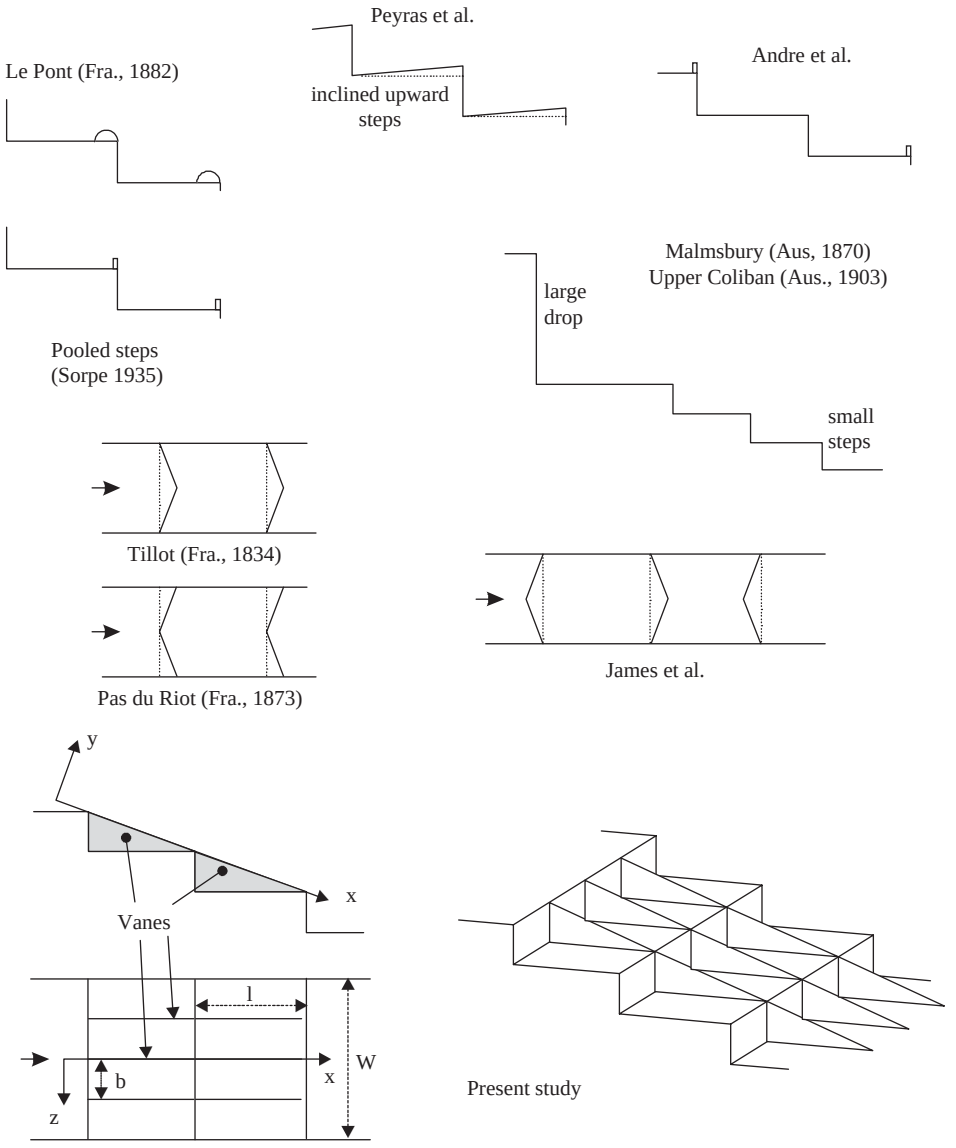

Figure 2. Examples of step configurations for energy dissipation enhancement.

Gold Creek dam, Titicus dam), but some were equipped with devices to enhance energy dissipation. Some spillways had pooled steps with vertical walls (Sorpe dam, 1932) or rounded edges (Le Pont dam, 1882) (Fig. 2). Recently ANDRE et al. (2001) suggested an alternance of pooled steps and flat steps for maximum energy dissipation. PEYRAS et al. (1991) demonstrated greater energy dissipation with inclined upward steps. All these techniques add considerable structural loads to the stepped structure and might not be economical.

Enhancement of energy dissipation may be provided by superposition of small and large steps. In Australia, the Malmsbury (1870) and Upper Coliban (1903) dam spillways were designed with a combination of large drops (h = 2 to 4 m) and stepped chutes (h = 0.305 m). At design flows, the drops operate with a nappe flow and the chutes in skimming flow regime. Their successful operation for more than a century suggests that the design is sound. On the model of the Kennedy's Vale dam (h/l = 1), STEPHENSON (1988) superimposed occasional large steps to smaller steps and he observed a 10% increase in energy dissipation for this model. JAMES et al. (2001) observed larger rates of energy dissipation with V-shaped step edges (Fig. 2). Two early French stepped spillways were also equipped with V-shaped steps: Tillot dam (1834) and Pas du Riot dam (1873). Both stepped spillways are still in use. CHANSON (2002b) argued however that step lateral deflections induce complicated three-dimensional flow patterns.

2 EXPERIMENTAL SETUP

New experiments were conducted at the University of Queensland in a 3.3 m long, 1 m wide, 21.8° slope chute previously used by CHANSON and TOMBES (2002). Waters were supplied from a large feeding basin (1.5-m deep, surface area 6.8 m × 4.8 m) leading to a sidewall convergent with a 4.8:1 contraction ratio. The test section consisted of a broad-crested weir (1 m wide, 0.6 m long, with upstream rounded corner (0.057-m radius)) followed by ten identical steps (h = 0.1 m, l = 0.25 m) made of marine ply. The stepped chute was 1 m wide with perspex sidewalls followed by a horizontal concrete-invert canal ending in a dissipation pit. For two series of experiments, the step cavities were equipped with vanes (Fig. 2, Table 1).

The flow rate was delivered by a pump controlled with an adjustable frequency AC motor drive, enabling an accurate discharge adjustment in a closed-circuit system. The discharge was measured from the upstream head above crest with an accuracy of about 2%. Clear-water flow depths were measured with a point gauge. Air–water flow properties were measured using a double-tip conductivity probe (⌀ = 0.025 mm) designed at the University of Queensland (CHANSON 1995). The probe sensors were aligned in the flow direction and excited by an air bubble detector

Table 1. Detailed experimental investigations of air entrainment on embankment dam stepped chutes.

Reference (1)	θ (deg.) (2)	q_w (m^2/s) (3)	h (m) (4)	Flow regime (5)	Instrumentation (6)	Remarks (7)
Chanson and Toombes (2002)	21.8	0.06 to 0.18	0.1	Transition, Skimming	Double-tip conductivity probe (⌀ = 0.025 mm)	L = 3.0 m. W = 1 m. Inflow: uncontrolled broad-crest. Experiments TC200.
	15.9	0.07 to 0.19	0.1	Transition, Skimming	Double-tip conductivity probe (⌀ = 0.025 mm)	L = 4.2 m. W = 1 m. Inflow: uncontrolled broad-crest. Experiments TC201.
Gonzalez and Chanson (2004)	15.9	0.020 to 0.200	0.05	Transition, Skimming	Double-tip conductivity probe (⌀ = 0.025 mm)	L = 4.2 m. W = 1 m. Inflow: uncontrolled broad-crest. Experiments CG202.
		0.075 to 0.220	0.10	Transition, Skimming		Incl. detailed measurements between step edges.
Present study	21.8	0.10 to 0.22	0.1	Skimming	Double-tip conductivity probe (⌀ = 0.025 mm)	L = 3.3 m. W = 1 m. Inflow: uncontrolled broad-crest. Experiments CG203.
				Type 1		b = W = 1 m (no vane).
				Type 2		b = W/4 = 0.25 m (3 vanes).
				Type 3		b = W/8 = 0.125 m (7 vanes).

Notes: b: spacing between vanes; L: chute length; W: chute width.

(UQ82.518). The probe signal was scanned at 20 kHz for 20 seconds. The translation of the probes in the direction normal to the channel invert was controlled by a fine adjustment traveling mechanism connected to a Mitutoyo™ digimatic scale unit (Ref. No. 572-503). The error on the vertical position of the probe was less than 0.025 mm. The accuracy on the longitudinal probe position was estimated as $\Delta x < \pm 0.5$ cm. The accuracy on the transverse position of the probe was less than 1 mm. Flow visualisations were conducted with high-shutter speed digital still- and video-cameras.

2.1 *Data processing*

The basic probe outputs were the void fraction, bubble count rate, velocity, turbulence intensity and air/water chord size distributions (e.g. CHANSON 2002a). The void fraction C is the proportion of time that the probe tip is in the air. The bubble count rate F is the number of bubbles impacting the probe tip. The bubble chord times provide information on the air-water flow structure. With a dual-tip probe design, the velocity measurement is based upon the successive detection of air-water interfaces by two tips. In turbulent air-water flows, the detection of all bubbles by each tip is highly improbable and it is common to use a cross-correlation technique (e.g. CROWE et al. 1998). The time-averaged air-water velocity equals: $V = \Delta x/T$, where Δx is the distance between tips and T is the time for which the cross-correlation function is maximum. The turbulent intensity $Tu = u'/V$ may be derived from the broadening of the cross-correlation function compared to the auto-correlation function (CHANSON and TOOMBES 2002):

$$Tu = 0.851 \times \frac{\sqrt{\Delta T^2 - \Delta t^2}}{T} \quad (1)$$

where ΔT as a time scale satisfying: $R_{xy}(T + \Delta T) = 0.5 \times R_{xy}(T)$, R_{xy} is the normalised cross-correlation function, and Δt is the characteristic time for which the normalised autocorrelation function R_{xx} equals 0.5. The autocorrelation function itself provides some information on the air-water flow structure. A time series analysis gives further information on the frequency distribution of the signal which is related to the air&water (or water&air) length scale distribution of the flow.

Chord sizes may be calculated from the raw probe signal outputs. The results provide a complete characterisation of air and water chord streamwise distribution and may be analysed in terms of particle clustering and grouping. CHANSON and TOOMBES (2002) considered two air bubbles to form parts of a cluster when the water chord separating the bubbles is less than one tenth of the mean water chord size. The measurement of air-water interface area is a function of void fraction, velocity, and bubble sizes. For any bubble shape and size distribution, the specific air-water interface area a defined as the air-water interface area per unit volume of air and water may be derived from continuity: $a = 4 \times F/V$.

2.2 *Stepped configuration*

Experimental observations highlighted the three-dimensional nature of recirculation vortices in the step cavities beneath the pseudo-bottom formed by the step edges. In absence of vane (see below), three to four cavity recirculation cells were observed across the channel width. The finding was consistent with similar observations by MATOS (Pers. Comm.) and YASUDA (Pers. Comm.) on steeper slopes. In the present study, three stepped geometries were tested systematically. All had ten identical flat horizontal steps. In the first configuration, no vane was installed. In the second and third geometries, vanes were placed across the step cavity from steps 2 to 10 as illustrated in Figures 2 and 3. The second and third configurations had 3 and 7 vanes respectively (Table 1, Fig. 3). The vanes were made of aluminum, with few in perspex next to the sidewall for flow visualisation. The vanes did not interfere with the free-stream.

Experimental observations were conducted for flow rates ranging from 0.1 to 0.22 m^3/s corresponding to a skimming flow regime (Table 1, column 5). Measurements were performed at step edges and between adjacent step edges (i.e. above the recirculation cavity).

3 BASIC AIR-WATER FLOW RESULTS

In skimming flows, the flow was smooth and no air entrainment occurred at the upstream end of the cascade. After a few steps the flow was characterised by strong air entrainment. Downstream

the two-phase flow behaved as a homogeneous mixture and the exact location of the interface became undetermined. There were continuous exchanges of air-water and of momentum between the main stream and the atmosphere, while intense cavity recirculation was observed. The mainstream air-water flow consisted of a bubbly flow region ($C < 30\%$), a spray region ($C > 70\%$) and an intermediate flow structure for $0.3 < C < 0.7$.

At inception of free-surface aeration, the flow was rapidly varied. Side view observations suggested that some air was entrapped by a flapping mechanism in the step cavity(ies) upstream of the visual location of free-surface aeration. In presence of vanes, aeration of two to three cavities were seen upstream of inception: that is, more than in absence of vanes for identical flow rates. Flow visualisations next to the chute sidewall and next to the inception point of free-surface aeration highlighted the effects of vanes onto cavity recirculation. Although the vanes did not interfere with the stream flow, they were subjected to strong transverse pressure forces: i.e., in the horizontal direction z normal to the stream flow direction. The pressure load fluctuations appeared to be of the same period and in phase with cavity fluid ejections described by CHANSON et al. (2002).

3.1 *Void fraction and velocity distributions*

Detailed measurements of void fraction and air-water velocity were conducted downstream of air entrainment inception. For the stepped configurations with vanes, measurements were conducted systematically at $z = 0$, b/4 and b/2, where z is the transverse direction with $z = 0$ on the channel centreline above a series of vanes and b is the spacing between vanes (Fig. 2).

For all stepped configurations, air concentration distributions highlighted smooth profiles that followed closely an analytical solution of the bubble advective diffusion equation. Between step edges, strong aeration was recorded in the step cavities. The results showed little effects of the vanes on the void fraction results (Fig. 4). Figure 4 presents typical dimensionless distributions of air concentrations C and velocity V/V_{90} at step edge, where V_{90} is the characteristic velocity at $y = Y_{90}$, y is the distance normal to the pseudo-bottom formed by the step edges and Y_{90} is the distance where $C = 0.9$. In Figure 4, the mean air content C_{mean} was 0.36 (no vane), 0.33 (7 vanes, $z/b = 0$) and 0.37 (7 vanes, $z/b = 0.5$).

Velocity measurements demonstrated that the effect of vanes extended far into the main stream. The velocity distributions showed some marked difference with 3 and 7 vanes for $y/Y_{90} < 0.6$ to 0.7 at all transverse positions ($z/b = 0$, 0.25 & 0.5). This is illustrated in Figures 4 and 5. Figure 5 shows typical dimensionless distributions of velocity V/V_{90} and turbulence intensity Tu between step edges. Data for $y < 0$ were recorded in the step cavity. Velocity measurements between step edges highlighted further the developing mixing layer downstream of each step edge (GONZALEZ and CHANSON 2004). Above vanes, the mainstream turbulence levels were usually lower than between vanes and than in absence of vanes.

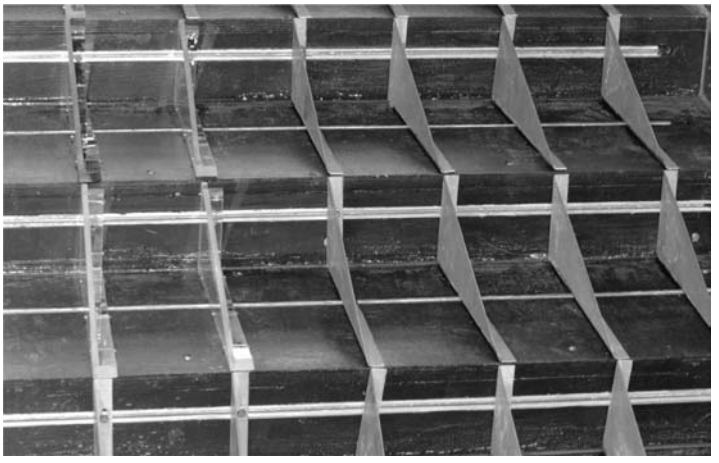

Figure 3. Photograph of the stepped invert with 7 vanes (Configuration 3).

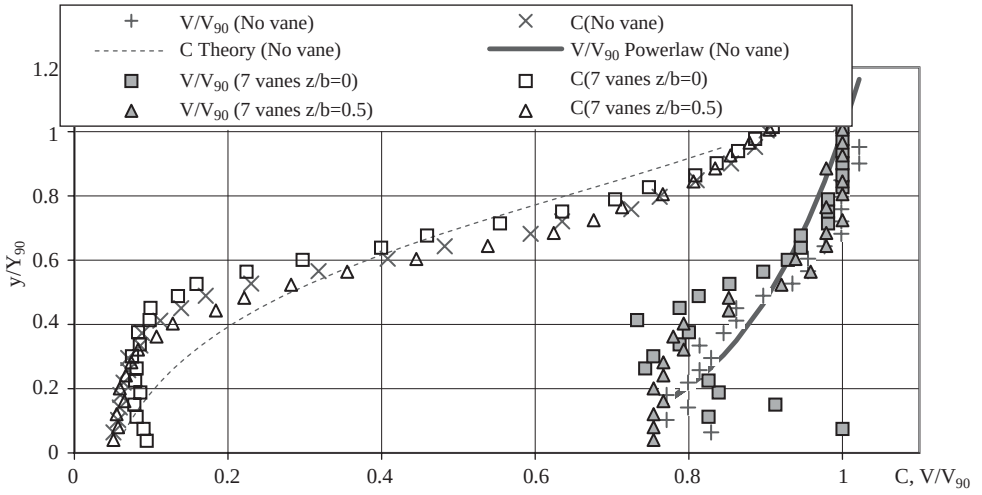

Figure 4. Dimensionless distributions of air concentrations and velocity at step edge 9 ($d_c/h = 1.5$) – Comparison between Configuration 1 (no vane) and Configuration 3 (7 vanes, $z/b = 0$ & 0.5).

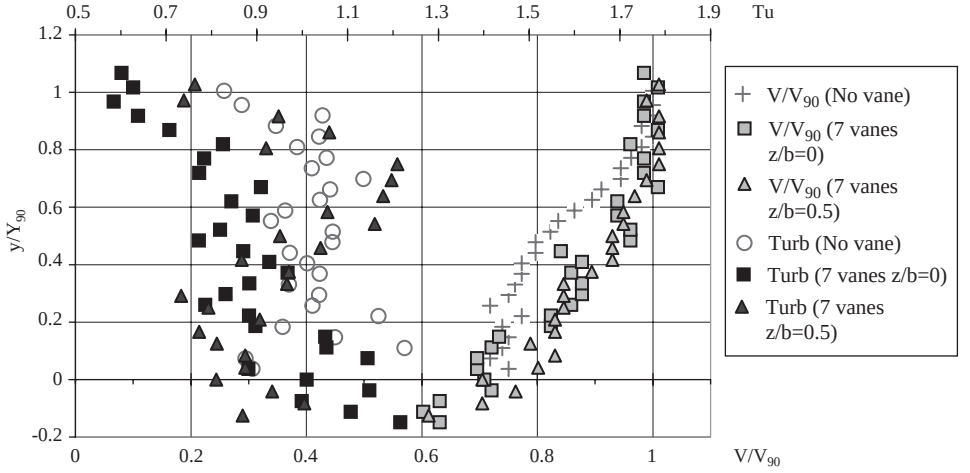

Figure 5. Dimensionless distributions of velocity and turbulence intensity at half-distance between step edges 9 and 10 ($d_c/h = 1.5$) – Comparison between Configurations 1 and 3 (7 vanes, $z/b = 0$ & 0.5).

3.2 *Flow resistance and energy dissipation*

Flow resistance was deduced from the average friction slope (e.g. CHANSON et al. 2002). For the stepped configurations with vanes, the flow resistance was calculated at $z/b = 0$ (above vane), $z/b = 0.25$ and $z/b = 0.5$. Results are presented in Table 2 for all configurations. In average they implied equivalent Darcy friction factors of about 0.25, 0.32 and 0.29 for no vane, 3 vanes and 7 vanes respectively suggesting that the presence of vanes increased the flow resistance and the rate of energy dissipation. It is believed that the vanes prevent the development of transverse turbulence in the cavities. The inhibition of large transverse vortical structures is associated with enhanced vertical mixing between recirculation zones and mainstream that is characterised by irregular fluid ejections, turbulent bursts and sweeps. Turbulent mixing enhancement yields greater rate of energy dissipation and flow resistance.

Table 2. Flow resistance estimates in air-water flows

	f_e						
		3 vanes			7 vanes		
d_c/h (1)	No vane (2)	z/b = 0 (3)	z/b = 0.25 (4)	z/b = 0.5 (5)	z/b = 0 (6)	z/b = 0.25 (7)	z/b = 0.5 (8)
1.1	0.234	0.355	0.304	0.337	–	0.297	0.301
1.3	0.244	0.340	0.318	0.314	–	0.312	0.293
1.5	0.281	0.373	0.301	0.272	0.281	0.31	0.273
1.7	0.249	0.408	0.287	0.259	–	0.273	0.259

4 SUMMARY AND DISCUSSION

In skimming flows on stepped channels, there is no skin friction between mainstream and step surfaces, but at the flow singularities generated by the step edges. Flow resistance is basically form drag. Alterations of flow recirculation and fluid exchanges between free-stream and cavity flow affect drastically form losses and in turn the rate of energy dissipation. This study presents a comprehensive series of air–water flow measurements on an embankment dam stepped chute. The introduction of vanes demonstrated simple turbulence manipulation and form drag modification that could lead to more efficient designs in terms of rate of energy dissipation without significant structural load on the chute.

However the design of embankment overflow stepped spillway is a critical process. Any single failure of the spillway system can lead to a total dam failure. A number of specific key issues must be assessed accurately and these include stepped chute operation and erosion, embankment seepage, drainage beneath steps, sidewall design (overtopping, scour), chute geometry (effects of chute convergence), and downstream energy dissipation and scour (CHANSON and TOOMBES 2001). Today some hydrodynamic processes are still inadequately understood. For example, the secondary currents at the connection between steps and (smooth) abutment walls, chute convergence effects, the interactions between seepage and free-surface flows, and downstream energy dissipation in a plunge pool. At the connection between steps and abutment walls, the differences in flow resistance between stepped invert and smooth concrete abutment generate transverse velocity gradient and secondary currents, associated with high shear forces. During overflows, seepage takes place in the embankment. Appropriate provision for drainage is required and drains are usually installed on the vertical face of the steps. With form drag, fluid injection in the separated region (i.e. the wake) does reduce drastically the drag (e.g. WOOD 1964, NAUDASCHER and ROCKWELL 1994). CHANSON and TOOMBES (2001) hypothesised that a similar mechanism may exist in skimming flows above embankment stepped spillway. At the downstream end of the spillway, submerged steps may be damaged during high tailwater level conditions. BAKER (2000) observed major damage to stepped block spillway sections submerged by a hydraulic jump and a plunge pool. YASUDA and OHTSU (2000) investigated the characteristics in the plunge pool downstream of a stepped chute as a function of the tailwater level. Although their results did not include efforts on the submerged steps, they observed some energy dissipation contribution from the submerged steps, suggesting some loads on the steps.

In most cases, physical modeling of embankment stepped spillway is strongly advised. Physical models are usually based upon a Froude similitude, but recirculation flows and free-surface aeration may induce significant scale effects in small-size laboratory models. The geometric scaling ratio should be no greater than 10:1, and preferably less than 5:1.

ACKNOWLEDGMENTS

The writers thank Mr G. ILLIDGE for his assistance and Professor C.J. APELT his valuable advice. The second writer acknowledges the financial support of the National Council for Science and Technology of Mexico (CONACYT) and of the University of Queensland.

REFERENCES

ANDRE, S., BOILLAT, J.L., and SCHLEISS, A. (2001). "High velocity two-phase turbulent flow over macro-roughness stepped chutes: focus on dynamic pressures." *3rd Intl Symp. Environmental Hydraulics*, Tempe, 6 pages (CD-ROM).

BAKER, R. (2000). "Field Testing of Brushes Clough Stepped Block Spillway." *Intl Workshop on Hydraulics of Stepped Spillways*, Zürich, Switzerland, Balkema Publ., pp. 13–20.

CHANSON, H. (1995). "Air Bubble Entrainment in Free-surface Turbulent Flows. Experimental Investigations." *Report CH46/95*, Dept. of Civil Engrg., Univ. of Queensland, Australia, 368 pages.

CHANSON, H. (2001). "The Hydraulics of Stepped Chutes and Spillways." *Balkema*, Lisse, The Netherlands, 418 pages.

CHANSON, H. (2002a). "Air-Water Flow Measurements with Intrusive Phase-Detection Probes. Can we Improve their Interpretation?" *Jl of Hyd. Engrg.*, ASCE, Vol. 128, No. 3, pp. 252–255.

CHANSON, H. (2002b). "Enhanced Energy Dissipation in Stepped Chutes. Discussion." *Proc. Instn Civ. Engrs Water and Maritime Engrg*, UK, Vol. 154, No. 4, pp. 343–345 & Front cover.

CHANSON, H., and TOOMBES, L. (2001). "Experimental Investigations of Air Entrainment in Transition and Skimming Flows down a Stepped Chute. Application to Embankment Overflow Stepped Spillways." *Research Report No. CE158*, Dept. of Civil Eng., Univ. of Queensland, Brisbane, Australia, 74 pages.

CHANSON, H., and TOOMBES, L. (2002). "Air-Water Flows down Stepped Chutes: Turbulence and Flow Structure Observations." *Intl Jl of Multiphase Flow*, Vol. 27, No. 11, pp. 1737–1761.

CHANSON, H., YASUDA, Y., and OHTSU, I. (2002). "Flow Resistance in Skimming Flows and its Modelling." *Can Jl of Civ. Eng.*, Vol. 29, No. 6, pp. 809–819.

CROWE, C., SOMMERFIELD, M., and TSUJI, Y. (1998). "Multiphase Flows with Droplets and Particles." *CRC Press*, Boca Raton, USA, 471 pages.

DITCHEY, E.J., and CAMPBELL, D.B. (2000). "Roller Compacted Concrete and Stepped Spillways." *Intl Workshop on Hydraulics of Stepped Spillways*, Zürich, Switzerland, Balkema Publ., pp. 171–178.

GONZALEZ, C.A., and CHANSON, H. (2004). "Interactions between Cavity Flow and Main Stream Skimming Flows: an Experimental Study." *Can Jl of Civ. Eng.*, Vol. 31 (accepted for publication).

JAMES, C.S., MAIN, A.G., and MOON, J. (2001). "Enhanced Energy Dissipation in Stepped Chutes." *Water & Maritime Engineering, Proc. Instn. Civ. Engrs.*, UK, Vol. 148, No. 4, pp. 277–280.

NAUDASCHER, E., and ROCKWELL, D. (1994). "Flow-Induced Vibrations. An Engineering Guide." *IAHR Hydraulic Structures Design Manual No. 7*, Hydraulic Design Considerations, Balkema Publ., Rotterdam, The Netherlands, 413 pages.

PEYRAS, L., ROYET, P., and DEGOUTTE, G. (1991). "Ecoulement et Dissipation sur les Déversoirs en Gradins de Gabions." *Jl La Houille Blanche*, No. 1, pp. 37–47.

STEPHENSON, D. (1988). "Stepped Energy Dissipators." *Proc. Intl Symp. on Hydraulics for High Dams*, IAHR, Beijing, China, pp. 1228–1235.

SCHUYLER, J.D. (1909). "Reservoirs for Irrigation, Water-Power and Domestic Water Supply." *John Wiley & sons*, 2nd edition, New York, USA.

WEGMANN, E. (1922). "The Design and Construction of Dams." *John Wiley & Sons*, New York, USA.

WOOD, C.J. (1964). "The Effect of Base Bleed on Periodic Wake." *Jl Roy. Aer. Soc.*, Vol. 68, pp. 477–482.

YASUDA, Y., and OHTSU, I. (2000). "Characteristics of Plunging Flows in Stepped Channel Chutes." *Intl Workshop on Hydraulics of Stepped Spillways*, Zürich, Switzerland, Balkema Publ., pp. 147–152.